Structural evolution of Au nanoclusters: From planar to cage to tubular motifs

Xiaopeng Xing,[1] Bokwon Yoon,[2] Uzi Landman,[2] and Joel H. Parks[1]
[1]*Rowland Institute at Harvard, Cambridge, Massachusetts 02142, USA*
[2]*School of Physics, Georgia Institute of Technology, Atlanta, Georgia 30332-0430, USA*
(Received 11 July 2006; published 27 October 2006)

The evolution of structural motifs of gold cluster anions, Au_n^-, in the size range $n=11-24$ has been determined through a comparison of electron diffraction data with density functional calculations. The results provide clear evidence for a transformation from planar to three-dimensional structures in the range $n=12-14$, the development of cage structures for $n=16$ and 17, the appearance of a tetrahedral structure at $n=20$, and the emergence of a highly symmetric tubular structure for $n=24$.

DOI: 10.1103/PhysRevB.74.165423 PACS number(s): 61.14.−x, 64.70.Nd, 36.40.Mr

I. INTRODUCTION

The size-dependent evolutions of the structures and physical and chemical properties of finite nanoscale materials aggregates have been the subjects of continuing basic and applied research interests. In particular, recent experimental and theoretical investigations of gold cluster anions have presented a unique opportunity to correlate sizes and structures with catalytic reactivity on an atom-by-atom level. In these studies, relationships between cluster structures and catalytic activities have been explored for metal-oxide-supported gold nanoclusters, and for gas-phase Au_n^- clusters.[1–4]

Structure determination is one of the outstanding challenges of cluster science, and it has been approached in several ways. Structural determination via analysis of diffraction measurements is most desirable, since the scattering data is related to the spatial arrangement of the scattering atoms in a direct manner. However, until quite recently such methodology was not practiced because of experimental technical difficulties, and consequently one resorted to more indirect methods, mostly through theoretical analysis of photoelectron spectroscopic (PES) data.[5–8]

Electron diffraction measurements, which may be regarded as a direct structural determination method,[9] allow for a comparison between the experimentally measured data and theoretical calculations, insofar as the measured patterns are the Fourier transform of the pair correlation function and thus are directly related to atomic positions. Quite recently it has been demonstrated that trapped ion electron diffraction (TIED) measurements of mass selected metal clusters are particularly sensitive to size-dependent changes in structural symmetries[10] and changes in local order.[11] This paper presents direct structural determination of gold structures, achieved through joint diffraction measurements and density functional calculations of gold cluster anions Au_n^- in the size range $11 \leqslant n \leqslant 24$. Through these investigations we identify specific ground state and isomeric structures and follow the remarkable size-dependent structural evolution among different symmetries and forms. Our analysis shows clear evidence of a planar [two-dimensional (2D)] to three-dimensional (3D) transition over the range $n=12-14$, caged structures for $n=16$ and 17, the development of a tetrahedral structure at $n=20$, and the emergence of a highly symmetric tubular structure at $n=24$. These results are in general agreement with those obtained through recent (PES/DFT) studies (see in particular Ref. 7 for a study of Au_n^-, $n=15-19$, and Ref. 8 for $n=15-24$).

II. METHODS

The trapped ion electron diffraction apparatus used in these experiments has been described elsewhere.[11] Electron diffraction is performed by irradiating a trapped cloud of $\sim 10^4$ mass selected cluster ions with a 40 kV electron beam carrying a current of ~ 0.6 μA. The clusters are relaxed to the temperature of the trap (~ 120 K) by collisions with a cold He background gas at ~ 120 K. The clusters are annealed by applying an external rf field ($V_{0-p} \sim 0.2$ V) for ~ 100 ms to excite translational motion, which heats the clusters by translational to vibrational (T-V) energy transfer in collisions with a background Ne gas ($\sim 10^{-3}$ torr). After annealing, the cluster ensemble is cooled to the He gas ($\sim 5 \times 10^{-3}$ torr) temperature over $\sim 3-5$ s. Clusters prepared in this way minimize the effects of cluster source parameters on the measured cluster structure. To obtain acceptable signal/noise, a typical experimental run of over ~ 10 h is required. The resulting diffraction pattern is an average over $\sim 1 \times 10^7$ mass selected clusters.

The electronic and geometric structures of the gold cluster anions were obtained through the use of the Born-Oppenheimer (BO) local spin-density-functional (LSD) molecular dynamics (MD) simulation method (BO-LSD-MD),[12] which was used as a tool for structural optimization via energy minimization using a technique similar to the conjugate-gradient method. In the calculations we employed norm-conserving scalar relativistic pseudopotentials[13] for the $5d^{10}6s^1$ valence electrons of the gold atom, within the generalized gradient approximation (PBE/GGA).[14] The Kohn-Sham (KS) orbitals were expanded in a plane-wave basis with a 62 Ry kinetic energy cutoff. This approach has been used by us in numerous occasions previously and its feasibility and accuracy for gold has been well documented.[15–17] The BO-LSD-MD method is particularly suited for studies of finite charged systems because it does not employ a supercell (periodic replication of the atoms), thus allowing for accurate determination of the total energy of both charged and neutral systems. All the clusters were relaxed fully without any sym-

metry constraints. A large number of initial structural candidates were used, but here we report only the few energetically low-lying isomers for each size, which are important in interpreting the experimental data.

The data was fit to a model of the total scattering intensity, I_{total}, approximated by the sum of independent scattering terms, I_{indep}, from each cluster atom and terms resulting from the interference of elastic scattering from atomic pairs. Multiple scattering processes do not contribute significantly for clusters in the size range explored in this study. The data analysis extracts the interference, or molecular scattering, contribution to the total scattering intensity by approximating the independent scattering contribution by a polynomial in s, the momentum transfer.[10,11,18] The momentum transfer is related to the scattering angle, θ, by $s=(4\pi/\lambda)\sin(\theta/2)$ where $\lambda=0.06$ Å is the de Broglie wavelength for 40 keV electron energy. The resulting molecular scattering intensity is defined by $sM(s)=s(I_{total}-I_{indep})/I_{indep}$ where I_{indep} is proportional to the atomic scattering factor. Broadening of the theoretical diffraction pattern by a factor $\sim\exp(-L^2s^2/2)$ (Ref. 19) was included in the fit to represent atomic vibrations in the cluster structure at finite temperature. This form of the temperature dependence is derived in the harmonic oscillator approximation and corresponds to the Debye-Waller factor associated with the scattering of phonon modes in solids. The mean squared vibrational amplitude, L^2, is taken to be the average over all atom pairs in the cluster. The data for each cluster size was fit to all theoretical isomer structures calculated for that size. These fits were performed with two different algorithms and in each case the same isomer structure was identified as the best fit with weighted R values[20] in the range of 0.07–0.10. The R value characterizes the fit between the weighted theoretical, $M^{\text{th}}(s)$, and experimental, $M^{\text{exp}}(s)$ values and is defined by

$$R=\left[\frac{\sum_i w_i(sM_i^{th}-sM_i^{\text{exp}})^2}{\sum_i w_i(sM_i^{\text{exp}})^2}\right]^{1/2}. \quad (1)$$

The sums are over all the data points, and the weighting factors are given as $w_i=1/\sigma_i^2$ where σ_i is the standard deviation for each raw data point, $I_{\text{tot},i}$. In the cluster size range on which we focus in this study, the signal-to-noise ratio in the displayed diffraction patterns degrades after $s\sim 7$ Å^{-1} and rapidly varying structure is a consequence of noise fluctuations and should be disregarded.

III. RESULTS AND DISCUSSION

The comparisons of diffraction data for annealed clusters with calculated structural isomers are shown in Figs. 1 and 2. For each cluster size, several calculated structures are shown at the top with the corresponding molecular intensity $sM(s)$ patterns for each isomer. At the bottom, the experimental data is compared with the calculated $sM(s)$ for the isomer structure producing the best fit. The experimental uncertainty shown includes only the standard deviations of the raw data. In several cases, the best fit diffraction pattern was derived by summing two patterns calculated for different isomeric structures. This sum of isomer contributions is assumed to represent an ensemble of trapped clusters composed of these structures. The fitting procedure varied the fractional contribution of each isomer structure in the $sM(s)$ model to optimize the fit to the experimental patterns.

In Fig. 1 we display a selection of calculated low-energy structures with associated molecular scattering intensities and diffraction data with best fits for clusters in the size range Au_n^- $11\leqslant n\leqslant 16$. Anionic gold clusters in this range have been the subject of theoretical[17,21] and experimental[22] discoveries identifying the presence of large planar clusters. Experimental evidence for a transition from planar to 3D structures has been observed in measurements of cluster ion mobility[22] at $n=12$ and photoelectron spectra[6] at $n=13$. As indicated in Fig. 1, theory predicts many low-lying isomers within ~0.3 eV for each cluster size. In cases for which the diffraction patterns do not clearly differentiate a particular structural isomer, ion mobility[22] and/or photoelectron measurements[6] can help to identify the most probable structure. Although different cluster sources can introduce uncertainty in the isomer distribution, it is nevertheless interesting to note cases in which the different measurements agree or are clearly inconsistent.

The Au_{11}^- diffraction pattern appears to be most consistent with the two lowest energy 2D isomers. The mobility measurement identifies the ground state structure (marked as 11G in Fig. 1). The Au_{12}^- diffraction pattern is best fit by a cluster ensemble composed of a mixture of two isomers: 54% planar ground state and 46% of 12II, which is the lowest 3D isomer. Both ion mobility and photoelectron measurements indicate an isomer mixture. This size appears to be the first departure from pure planar structure. The best fit of the Au_{13}^- diffraction data also appears to arise from a mixture of structural isomers: 20% planar ground state and 80% of 13I (the lowest energy 3D structure). Ion mobility observes a nonplanar structure and also suggests the 3D isomer 13I, whereas the photoelectron results indicate the presence of an isomer mixture. For Au_{14}^-, there is no evidence of a planar structure and the diffraction pattern is best fit by a single isomer, the lowest energy 3D structure 14I, in agreement with both mobility and photoelectron data. The diffraction pattern for Au_{15}^- is best fit by the higher lying isomer 15VI. The theoretical pattern is unique among the eight isomer patterns calculated for Au_{15}^- providing support for this assignment (isomers II and III not shown). The photoelectron spectra suggest a mixture of the 15III and 15V isomers, which is inconsistent with the diffraction result. In summary, the above patterns depict a transition with cluster size from planar to 3D structures. The smooth nature of the transition is reflected by the occurrence of sets of closely spaced-in-energy isomers for cluster sizes in the transition region ($n=12-14$).

Calculated structures with associated molecular scattering intensities and diffraction data with best fits for Au_n^- in the size range $16\leqslant n\leqslant 21$ and $n=24$ are shown at the bottom of Fig. 1 ($n=16$) and in Fig. 2. The diffraction pattern for Au_{16}^- is uniquely fit by the cage structure isomer 16I lying 0.08 eV above the 2D ground state. Evidence for this cage structure

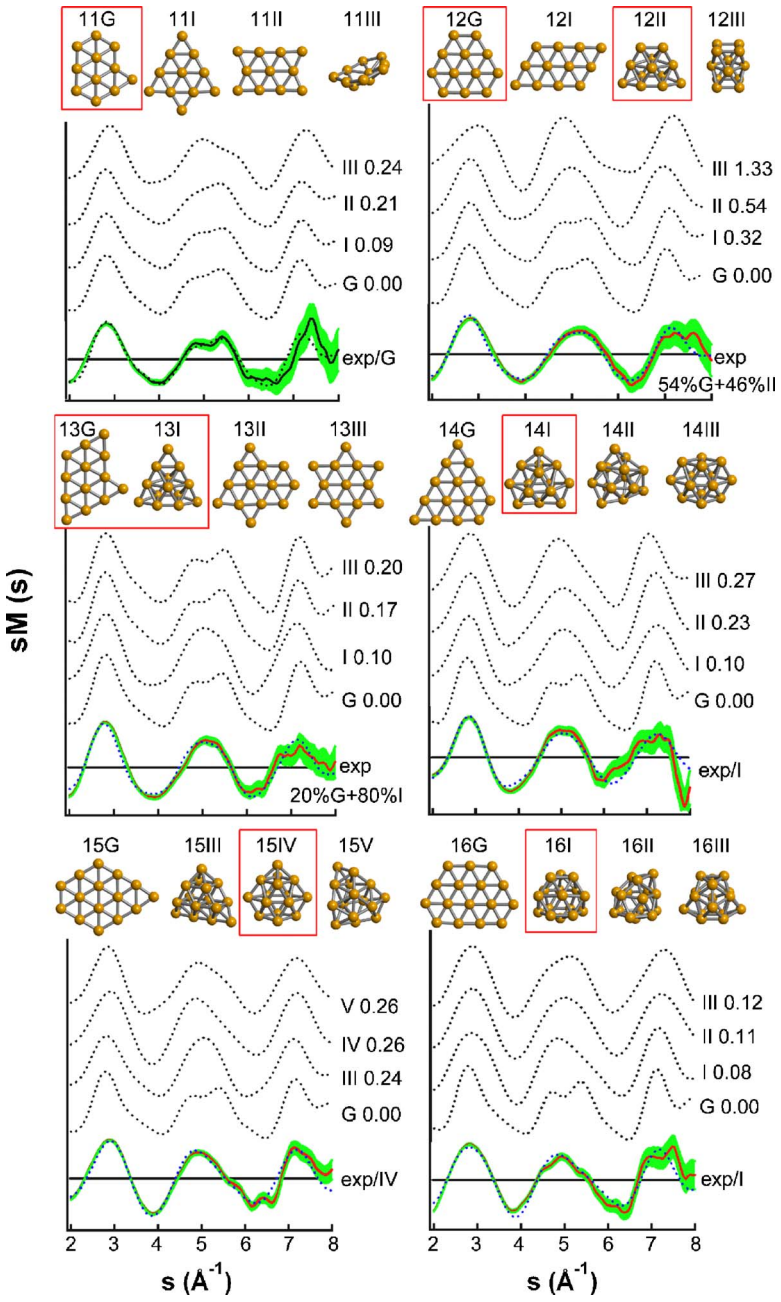

FIG. 1. (Color online) Calculated isomer structures for Au_n^- clusters with $11 \leqslant n \leqslant 16$ are shown at the top of each panel with corresponding diffraction patterns of $sM(s)$ vs s (A^{-1}) depicted below (dotted curve). Experimental diffraction $sM(s)$ (solid curve, online red) along with the best fit (dotted curve, online blue) are shown at the bottom. The gray (online green) shading shows the data uncertainty $\pm\sigma$. The energy of the isomer above that of the ground state (GS) is shown on the right for each isomer. The diffraction intensity has arbitrary units. The isomers that constitute the best fit are marked by a red frame in each panel.

has recently been observed in photoelectron measurements.[7] The diffraction pattern for Au_{17}^- is fit equally well by the ground state cage structure and a second low-energy isomer separated by only 0.06 eV. However, the photoelectron results[7] prefer the ground state cage structure. The diffraction pattern for Au_{18}^- is best fit by the isomer 18I that lies only 0.02 eV above the ground state. The theoretical diffraction pattern for this fit is unique among the six isomer patterns calculated for Au_{18}^-, providing strong evidence for assigning the 18I structure. The photoelectron spectra suggest a mixture of the ground state and the 18IV isomer which is inconsistent with the diffraction result.

The diffraction patterns observed for clusters in the size range $n=18-20$ all exhibit a shoulder on the left side of the second peak, which is evidence for the presence of fcc symmetry (which is the bulk gold structure). This symmetry has been identified[5] for the tetrahedral structure of the Au_{20}^- ground state, which gives the best fit to the diffraction pattern. The diffraction pattern for Au_{19}^- is also fit by a similar tetrahedral structure (the ground state structure 19G) in which a single vertex atom is missing. The structure for Au_{18}^-, 18I, which provides the best fit with the diffraction data, is also related to the tetrahedral structure with atoms missing at two vertices and slight atomic displacements. However, with the addition of a single atom—that is, for Au_{21}^-—the observed diffraction pattern changes in a radical fashion. Although there are several low-energy structures for Au_{21}^- that display the presence of fcc symmetry, the best fit structure is found to be isomer 21IV, an elongated cage.

Figure 2 displays also the diffraction pattern and calculated structures for Au_{24}^-, that present evidence for the emergence of an empty single-wall tubelike structure.[23] Indeed,

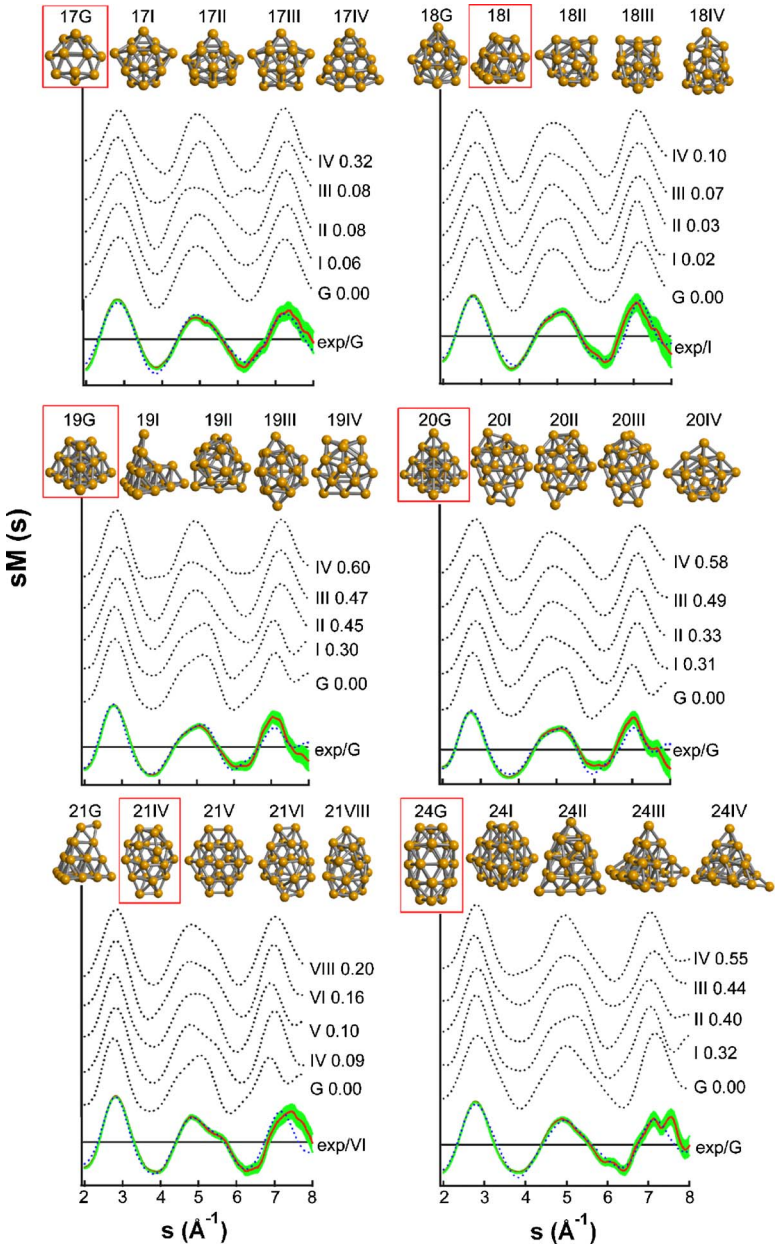

FIG. 2. (Color online) Similar to Fig. 1 for diffraction data and isomer structures for Au_n^- clusters with $17 \leqslant n \leqslant 21$ and $n=24$.

the best fit structure is found to be the highly symmetric ground state isomer, 24G, whose structure (shown in Fig. 3, second image from the left) is composed of three stacked six-member rings with the center one (dark gray balls, online green) being hexagonal and the other two having threefold symmetry (black balls, online red). The outer six-member rings are each capped by a three-atom triangle (light gray balls, online yellow) as shown in Fig. 3. The commonality between the Au_{24}^- and Au_{16}^- structures is also shown in Fig. 3, where we note that both these low-energy structures contain 12 atoms with fivefold coordination and 12 (4 for Au_{16}^-) atoms with sixfold coordination. Figure 3 also indicates that the tubular structure of Au_{24}^- may be viewed as obtained from the 16I isomeric structure of Au_{16}^- by replacing the bottom capping atom in the latter by a six-member ring, which is then capped by a triangle. The diffraction patterns for $n=16$ and 24 are essentially identical and unique among all the patterns derived from the calculated isomers, both exhibiting a triangular second peak, which supports our structural assignments.

IV. SUMMARY

We have reported here on electron diffraction measurements and first-principles theoretical analysis of the size-dependent evolution of structural motifs found in gold anion clusters, Au_n^-, in the size range $n=11-24$ atoms. The identification of these structures has been accomplished through direct structural determination—that is, the comparison of electron diffraction data from trapped clusters with density functional calculations of structural isomers for each cluster size (see also Ref. 8). The structural evolution that we have described exhibits changes in dimensionality and symmetry, with the clusters evolving from planar species at $n=11$ (and smaller ones) to three-dimensional structures in the range $n=12-14$, to hollow cages for $n=16$ and 17, followed by the

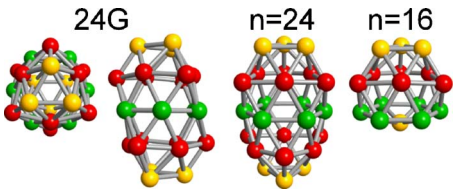

FIG. 3. (Color online) The ground state tubular structure of Au_{24}^- is shown (on the left) in end-on and perspective views to emphasize the symmetry aspects of the structure. A comparison of the structures of gold cluster anions with $n=24$ and $n=16$ atoms is also shown on the right. The tubular structure is seen best in the second and third images from the left, and it consists of three stacked six-member rings with the center one (dark gray balls, online green) being hexagonal and the other two having threefold symmetry (black balls, online red). The outer six-member rings are each capped by a three-atom triangle (light gray balls, online yellow).

appearance of a tetrahedral structure at $n=20$, and the emergence of a highly symmetric tubelike structure at $n=24$.

The rich array of size-dependent structural motifs described in this study is specific to gold clusters and it is likely to originate from the relativistically enhanced *s-d* hybridization of gold bonding orbitals.[17] The determination of these cluster structures, achieved here through joint electron diffraction measurements and first-principles calculations, adds to the published plethora of gold structures (see Refs. 5–8, 15–17, and 21–23 and representative articles in Ref. 24). Most importantly, the determination of these cluster structures is essential to an understanding of the size-dependent evolution of cluster properties; for example, assisting in gaining a more complete understanding of the mechanisms that control the chemical reactivity and catalytic activity of gold clusters.[25]

ACKNOWLEDGMENTS

UL and BY thank P. Koskinen, B. Huber, O. Kostko, B. von Issendorf, H. Häkkinen, and M. Moseler, their coauthors in Ref. 8, for collaboration on the theoretical determination of the structures of the gold clusters shown in this work. JHP was supported by the Department of Energy (DOE) under Grant No. DE-FG02-01ER45921. UL and BY were supported by the AFOSR and the U.S. DOE. Computations were performed at the Georgia Tech Center for Computational Materials Science and at NERSC, Berkeley, California.

[1] A. Sanchez, S. Abbet, U. Heiz, W.-D. Schneider, H. Häkkinen, R. N. Barnett, and U. Landman, J. Phys. Chem. A **103**, 9573 (1999).

[2] H. Häkkinen, S. Abbet, A. Sanchez, U. Heiz, and U. Landman, Angew. Chem., Int. Ed. **42**, 1297 (2003).

[3] B. Yoon, H. Häkkinen, U. Landman, A. S. Wörz, J.-M. Antonietti, S. Abbet, K. Judai, and U. Heiz, Science **307**, 403 (2005).

[4] B. Yoon, H. Häkkinen, and U. Landman, J. Phys. Chem. A **107**, 4066 (2003).

[5] J. Li, X. Li, H.-J. Zhai, and L.-S. Wang, Science **299**, 864 (2003).

[6] H. Häkkinen, B. Yoon, U. Landman, X. Li, H.-J. Zhai, and L.-S. Wang, J. Phys. Chem. A **107**, 6168 (2003).

[7] S. Bulusu, X. Li, L.-S. Wang, and X. C. Zeng, Proc. Natl. Acad. Sci. U.S.A. **103**, 8326 (2006).

[8] B. Yoon, P. Koskinen, B. Huber, O. Kostko, B. von Issendorf, H. Häkkinen, M. Moseler, and U. Landman, Phys. Chem. Chem. Phys. (to be published). The structures developed in this paper (for Au_n^- clusters with $15 \leqslant n \leqslant 24$) and used for interpretation of PES data, were employed in the current study in analysis of the TIED measurements. The two analyses were carried out independently of each other and the structural determinations are in overall excellent agreement.

[9] We remark that the term "direct structural determination method" is used here to signify a method that is based on a diffraction process, and to distinguish such method from those that while measuring properties that are structure-sensitive (for example, electron spectroscopy), are not based on scattering and/or diffraction from the atomic constituents. This does not imply that in a direct structural determination method further analysis of the data, including comparisons between the measured diffraction patterns and those calculated for theoretically optimized structures, is not required in order to fully determine the atomic arrangement.

[10] S. Krückeberg, D. Schooss, M. Maier-Borst, and J. H. Parks, Phys. Rev. Lett. **85**, 4494 (2000).

[11] X. Xing, R. M. Danell, I. L. Garzón, K. Michaelian, M. N. Blom, M. M. Burns, and J. H. Parks, Phys. Rev. B **72**, 081405(R) (2005).

[12] R. N. Barnett and U. Landman, Phys. Rev. B **48**, 2081 (1993).

[13] N. Troullier and J. L. Martins, Phys. Rev. B **43**, 1993 (1991).

[14] J. P. Perdew, K. Burke, and M. Ernzerhof, Phys. Rev. Lett. **77**, 3865 (1996).

[15] H. Häkkinen and U. Landman, Phys. Rev. B **62**, R2287 (2000).

[16] H. Häkkinen and U. Landman, J. Am. Chem. Soc. **123**, 9704 (2001).

[17] H. Häkkinen, M. Moseler, and U. Landman, Phys. Rev. Lett. **89**, 033401 (2002).

[18] D. Schooss, M. N. Blom, J. H. Parks, B. v. Issendorf, H. Haberland, and M. M. Kappes, Nano Lett. **5**, 1972 (2005).

[19] L. S. Bartell, D. A. Kohl, B. L. Carroll, and R. M. Gavin Jr., J. Chem. Phys. **42**, 3097 (1965).

[20] E. Prince, in *The Rietveld Method*, edited by R. A. Young (Oxford University Press, Oxford, 1995), p. 43.

[21] S. Gilb, Ph.D. thesis, University of Karslruhe, 2001.

[22] F. Furche, R. Ahlrichs, P. Weis, C. Jacob, S. Gilb, T. Bierweiler, and M. M. Kappes, J. Chem. Phys. **117**, 6982 (2002).

[23] Recently, tubelike structures were predicted [W. Fa and J. Dong, J. Chem. Phys. **124**, 114310–1 (2006)] for Au_{26} to Au_{28} neutral clusters with atoms having fivefold and sixfold coordination. However, there is no experimental evidence for these structures. We also note that supported single-shell gold nanowires exhibiting a tubelike helical structure have been reported in an electron microscope study[Y. Oshima, A. Onga, and K. Takayanagi,

Phys. Rev. Lett. **91**, 205503–1 (2003)].

[24] For an assortment of recent theoretical papers, based on density functional calculations, on the structures of neutral gold clusters with sizes outside the range of those investigated in the current paper, see M. P. Johansson, Angew. Chem., Int. Ed. **43**, 2678 (2004); X. Gu, M. Ji, S. H. Wei, and X. G. Gong, Phys. Rev. B **70**, 205401 (2004); H. Gronbeck and P. Broqvist, *ibid.* **71**, 073408 (2005); R. M. Olson, S. Varganov, M. S. Gordon, H. Metiu, S. Chretien, P. Piecuch, K. Kowalski, S. A. Kucharski, and M. Musial, J. Am. Chem. Soc. **127**, 1049 (2005); Y.-K. Han, J. Chem. Phys. **124**, 024316 (2006); E. M. Fernandez, J. M. Soler, and L. C. Balbas, Phys. Rev. B **73**, 235433 (2006).

[25] U. Heiz and U. Landman, *Nanocatalysis* (Springer, Berlin, 2006).